PHYSICAL REVIEW B VOLUME 27, NUMBER 10 15 MAY 1983

Localized modes and hydrogen trapping in niobium with substitutional impurities

D. Richter
Institut fur Festkörperforschung der Kernforschungsanlage Jülich, D-5170 Jülich, Federal Republic of Germany

J. J. Rush and J. M. Rowe
National Measurement Laboratory, National Bureau of Standards, Washington, D.C. 20234
(Received 27 December 1982)

The trapping of hydrogen by the substitutional impurities Ti and Cr in Nb has been investigated by neutron inelastic scattering measurements of hydrogen vibration spectra as a function of temperature. In the case of Ti, the hydrogen is in a trap which is deep enough to prevent precipitation into the hydride phase at low temperatures. In the trapped state, the hydrogen occupies a tetrahedral site which is likely to be a neighbor of the Ti impurity. The higher-energy vibrational-mode peak is shifted down by ≈ 10 meV and broadened somewhat with respect to that in pure niobium. In the case of Cr impurities the trap is shallower, and precipitation to the hydride phase is not inhibited at low temperatures. By studying the detailed behavior of the temperature dependence of the vibrational line shapes for dissolved, trapped, and precipitated H, a binding energy at the Cr trap of 105 ± 10 meV has been derived.

I. INTRODUCTION

The phenomenon of the trapping of hydrogen by various defects and impurities in metals has been the subject of considerable recent interest. Early thermodynamic measurements such as vapor pressure[1] and solubility[2] showed that trapping could occur at substitutional impurities and defects produced by cold working of the metal. Resistivity measurements[3] showed that in NbN_xH_y, precipitation of hydrogen into the hydride phase at low temperatures was completely suppressed for $y < x$, while internal-friction measurements[4] showed specific relaxation peaks related to hydrogen-impurity pairs. Quasielastic neutron scattering[5] allowed a direct probing of the trapping mechanism, which revealed complex capture and release processes which are a consequence of the spatial extent of the distorted region near an impurity.

Recent work has focused on the microscopic behavior of H in the trapped state. Internal-friction measurements on NbO_xH_y (Ref. 6) were interpreted in terms of various relaxation processes. Low-temperature specific-heat anomalies[7] were interpreted as evidence of H tunneling near the impurities, a view supported by ultrasonic attenuation measurements.[8] Neutron inelastic scattering[9] allowed the direct observation of a tunnel-split hydrogen ground state in NbO_xH_y at low temperatures. Quasielastic neutron scattering[10] revealed a local hopping process of the H near an O or N impurity in Nb at higher temperatures. However, in spite of all these measurements, the information on the local site symmetry of a trapped proton has remained either contradictory or nonexistent. In addition, a detailed knowledge of the trapping site and the potential between hydrogen and an impurity is required for a complete understanding of the trapping process and of the local dynamics of the trapped hydrogen.

Both of these problems can be addressed directly by neutron inelastic scattering studies of the vibrational states of the hydrogen. Such studies reveal two specific types of information.

(1) The *magnitude* of the vibrational frequencies gives direct information about the strength of the metal-hydrogen interaction and thus about the potential. In particular, for systems with impurities, the effects of lattice strains and/or local changes in the electronic environment can be probed.

(2) The *intensity* of the neutron scattering is directly related to the degeneracy of the given levels, which is in turn a direct consequence of the point symmetry of the interstitial position occupied. For example, in body-centered-cubic metals for both the octahedral and tetrahedral sites, one of the two fundamental levels is twofold degenerate. However, for the octahedral site it is the lower-energy level, while for the tetrahedral site it is the higher-energy level. For sites with lower symmetry (e.g., the triangular sites) all three fundamental energy levels are nonde-

 ©1983 The American Physical Society

generate. This sensitivity to the local environment of the hydrogen makes neutron spectroscopy a uniquely powerful tool in the assignment of the interstitial site occupied.[11]

In addition, trapping phenomena associated with changes of the vibrational energy levels of the hydrogens can be studied in detail by measuring the temperature dependence of the neutron scattering line shapes. The transfer of intensity from the free- to the trapped-energy level is directly related to the temperature dependence of the relative occupations of the two types of site, and hence to the trapping energy.

Recently, neutron inelastic scattering was used for the first time to study the vibrational spectra of hydrogen trapped by interstitial N and O impurities in Nb.[12] A surprising result of that study was that the impurities had only a small effect on the basic energy levels of the hydrogen vibrations. This, coupled with the observed degeneracy of the levels, led to the conclusion that the hydrogen was trapped in a relatively undistorted tetrahedral site in the vicinity of the impurity. In the same study it was shown that vanadium substitutional impurities below the 1% level did not prevent precipitation of a hydride phase at low temperatures. In this paper, we extend these measurements to a detailed study of trapping by the substitutional impurities Ti and Cr in Nb. These two elements were chosen for study because Cr causes the largest elastic distortion in Nb, and hence is expected to trap mainly by elastic interaction, while Ti has a large affinity for hydrogen, and hence may be expected to trap by electronic interactions. From the present study, in which the details of the temperature dependence of the various spectral components are studied for the first time, we are able to determine the binding energy of the trap associated with Cr from the temperature dependence of the occupation of the trap.

II. EXPERIMENTAL

The Cr- and Ti-doped polycrystalline Nb samples were produced by HF induction melting. Marz grade Nb with a nominal purity of 99.99% was used as a starting material. It was decarbonated and subsequently degassed in ultrahigh vacuum. The nominal purities of the alloying elements were Ti (99.999% purity) and Cr (99.99% purity). The actual dopant concentration was controlled by atomic absorption spectroscopy and yielded 0.899 ± 0.002 at. % Cr and 0.998 ± 0.021 at. % Ti. Hydrogen loading was performed from the gas phase and monitored by weight increase. The resultant H concentrations were 0.92 ± 0.02 at. % for the *Nb*Ti sample and 0.88 ± 0.03 at. % for the *Nb*Cr sample, in both cases slightly below the substitutional impurity concentrations.

The experiments were carried out on the BT-4 triple-axis spectrometer at the NBS research reactor. Cu 220 was used as a monochromator, and a Be filter at liquid-nitrogen temperature was utilized as an analyzer. The cold Be-filter analyzer combines a well-shielded detector (225 cm^2) with large vertical and horizontal divergence and yields a high signal-to-noise ratio. Applying a collimation of 40 min before and after the monochromator, the energy resolution varied between 6.5 meV full width at half-maximum (FWHM) at 100 and 9.5 meV at 170 meV energy transfer.

III. RESULTS

Figures 1 and 2 show spectra obtained on $NbTi_xH_y$ and $NbCr_xH_y$, respectively, at various temperatures. Figure 3 shows the detailed temperature dependence of the inelastic intensity around the lower-peak position studied for NbCrH. All spectra have been corrected for the fast neutron background. In addition, the scattering from the Nb metal was removed by subtracting a spectrum obtained from pure Nb. At room temperature *Nb*TiH exhibits a broad density-of-states distribution which peaks around 104 meV and shows only a weak broad feature at higher energies, close to that observed for

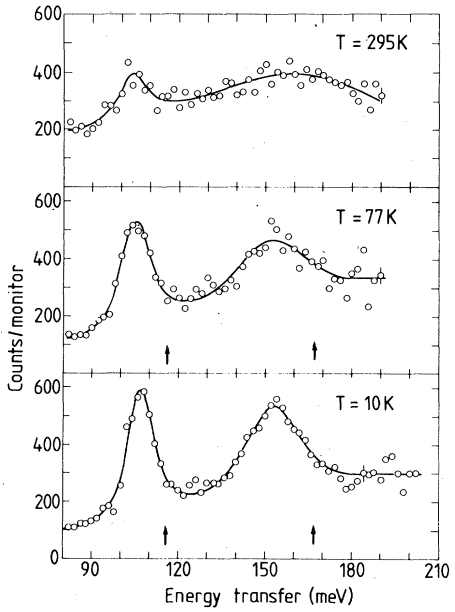

FIG. 1. Inelastic spectra obtained from $NbTi_{0.01}H_{0.009}$ at three temperatures. The arrows indicate the peak positions in the hydride phase (Refs. 13 and 14).

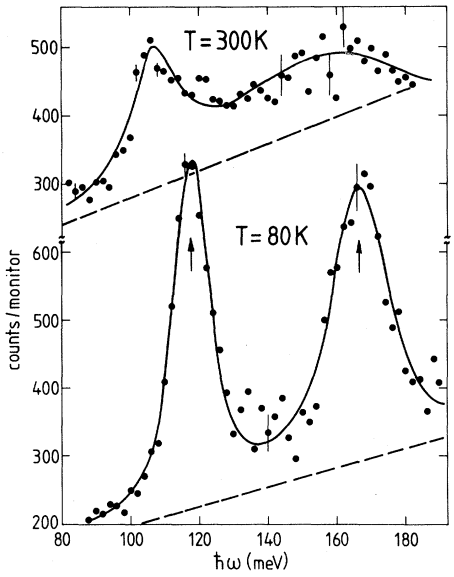

FIG. 2. Vibrational spectra obtained from $NbCr_{0.009}H_{0.009}$ at two temperatures.

α-$NbH_{0.005}$ and $NbV_{0.008}H_{0.005}$ in a previous study.[12] The position and width of the lower peak change relatively little with decreasing temperature. The higher fundamental, on the other hand, sharpens considerably with decreasing T and shifts by about 10 meV toward lower energies. At 10 K both frequencies are distinctly different from those in the ordered hydride phases (indicated by arrows in Fig. 1).

In *Nb*CrH the frequency distribution at room temperature is similar to that observed for *Nb*TiH. Again, we observe a very broad density of states with a lower fundamental at 106 meV, quite close to that observed for pure α-*Nb*H.[12] At 77 K both peaks are sharp and at the same energy as in the Nb-hydride phase. In Fig. 3 the intensity transfer from the high-temperature peak near 106 meV to higher energy peaks at lower temperatures is displayed. As can be seen, a second peak develops gradually at an energy of approximately 123 meV (T=250, 235, and 220 K). At 210 K separate peaks are not distinguishable, and we have a broad intensity distribution between 100 and 130 meV. Near 200 K a new center of vibrational density of state develops near 117 meV. At even lower temperatures, all of the intensity has shifted into this peak.

A. Data analysis and test of trapping models

Omitting optic and acoustic multiphonon contributions, the double differential neutron cross section for a three-dimensional harmonic oscillator for energy-loss processes has the form:

$$\frac{\partial^2\sigma}{\partial\omega\,\partial\Omega}=\frac{\sigma^{\mathrm{tot}}k_f}{4\pi k_i}\exp[-2W_b(Q)-2W_l(Q)]\times\sum_{n=1}^{3}\frac{\hbar Q^2}{6M\omega_n}\delta(\omega-\omega_n)\ , \tag{1}$$

where k_i and k_f are the momenta of the incoming and scattered neutron, $\vec{Q}=\vec{k}_i-\vec{k}_f$ is the momentum transfer at the sample, M is the mass of the proton, ω_n are the vibrational frequencies, σ^{tot} is the total H cross section, and W_b and W_l are the Debye-Waller factor contributions from the band and the local modes given, respectively, by

$$2W_b=\frac{\hbar^2Q^2}{M_n}\frac{3k_BT}{(k_B\Theta_D)^3}\ , \tag{2}$$

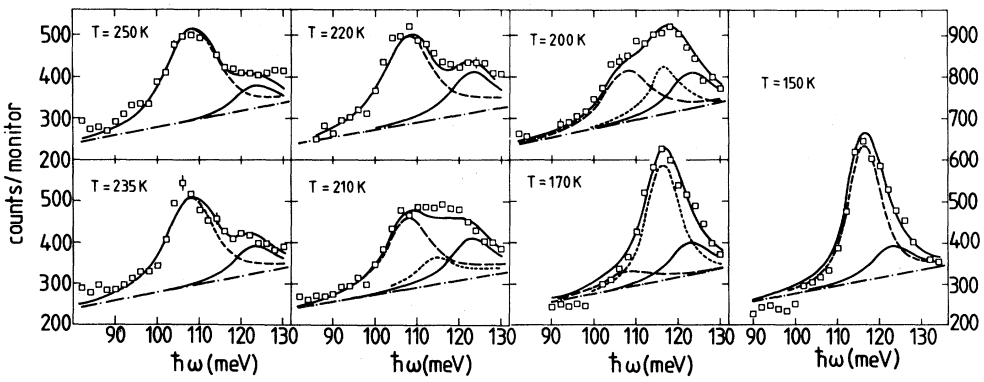

FIG. 3. Temperature dependence of the intensity distribution in the region of the lower fundamental vibration in $NbCr_{0.009}H_{0.009}$. The upper solid line represents the result of a fit with the combined trapping and precipitation model (see text). The broken line represents the α-phase contribution, the dashed line the intensity from protons in the hydride phase, while the lower solid line displays the intensity originating from protons in the trap. Finally, the dot-dashed line shows the background level.

$$2W_l=\frac{\hbar^2Q^2}{6m_{\mathrm{H}}}\sum_{i=1}^{3}\frac{1}{\hbar\omega_i}\coth\frac{\hbar\omega_i}{2k_BT} \quad . \tag{3}$$

In the above, Θ_D is the Debye temperature ($\Theta_D^{\mathrm{Nb}}=275$ K) and M_n is the mass of the host atoms. Since all experimental temperatures correspond to energies well below the local-mode energies, occupation of the ground state only has been assumed. For real systems, where the local H vibrations are broadened due to lifetime effects (anharmonicity) and lattice strains, the δ functions have to be replaced by intensity distribution functions. In what follows, we assume Lorentzian line shapes.

All of the data were first fitted to Eq. (1) (with the δ functions replaced by Lorentzians) convoluted with the instrumental resolution, where the Lorentzian widths, positions, and intensities were the fitting parameters. It should be noted that the exact widths extracted from this procedure would change considerably if one were to assume a different line shape (e.g., Gaussian). However, these results do provide a basis for comparison. The instrumental resolution was obtained by convolution of the monochromator resolution function with a Be transmission function assumed to be constant from 0.0 to 5.2 meV and zero elsewhere. The resultant peak positions and widths are listed in Table I, where the estimated errors are derived from the fitting procedure and do not include estimates of any possible systematic errors.

Next, the data for $NbCr_{0.009}H_{0.009}$ shown in Fig. 3 were fitted to three different models, each of which explained the intensity transfer in different ways. For each model, a different temperature dependence of the occupation of trapped sites was assumed and then all of the data for all temperatures were fitted *simultaneously,* with the constants describing the assumed temperature behavior as parameters. As described above, the models were convoluted with the resolution of the apparatus.

In the first model, only trapping was considered. In this case, we assume that the peak at 300 K represents the α-phase behavior while that at 80 K represents the trapped state (see Table I). The temperature dependence of the fractional occupations of these two states can be inferred from thermodynamic arguments.[3] In the simplest case, a trapping region near an impurity atom can be described as a number n of interstitial sites with potential energy reduced from unperturbed sites by an amount ΔE, the binding energy of the trap. In thermal equilibrium the chemical potentials of the dilute and trapped fractions are equal, so that

$$k_BT\ln(z_f/Z_f) = -\Delta E+k_BT\ln[(z_t/Z_t)(1-z_t/Z_t)^{-1}] \quad , \tag{4}$$

where z_f and z_t are the number of protons in the dilute and trapped states, respectively, and $Z_f=6Z_{\mathrm{Nb}}$ and Z_t are the available number of such sites. For the dilute protons blocking can be ignored, but in calculating the chemical potential for the trapped protons it cannot be. After some algebra, the concentration of trapped protons is given by

$$C_t=\tfrac{1}{2}\{C_{\mathrm{H}}+C_i+(6/n)e^{-\Delta E/k_BT} -[C_{\mathrm{H}}+C_i+(6/n)e^{-\Delta E/k_BT}]^2 -4C_{\mathrm{H}}C_i\}^{1/2} \quad , \tag{5}$$

where C_{H} and C_i are the hydrogen and impurity concentrations, respectively. In the above, we also assume that each impurity can trap only one hydrogen, as has been shown for N in Nb.[3] Using Eq. (5) with n and ΔE as fitting parameters, the result shown as $\tilde{C}_t$ in Fig. 4 was obtained. The prediction of this model, which shows a slow smooth variation of concentration, is inconsistent with the rapid intensity transfer observed in Fig. 3 between 220 and 200 K. This result is further supported by the fact that the spectrum observed at temperatures ≤ 150 K is virtually identical to that observed previously for ordered hydride phases in Nb.[12–14]

In the second model, we assume no trapping at all, i.e., that the observed intensity transfer is due only to hydrogen precipitation into the hydride phase. In this case, the maximum hydrogen concen-

TABLE I. Vibrational frequencies of H in $Nb\mathrm{Ti}_{0.01}\mathrm{H}_{0.009}$ and $Nb\mathrm{Cr}_{0.009}\mathrm{H}_{0.009}$.

Temperature (K)		$\hbar\omega_1$ (meV)	FWHM (meV)	$\hbar\omega_2$ (meV)	FWHM (meV)
*Nb*TiH	295	104.0±1.0	8.0±3.0		
	77	105.0±0.5	9.0±1.0	153.0±2.0	29.0±6.0
	10	107.0±0.5	7.0±1.0	153.0±1.0	20.0±2.0
*Nb*CrH	295	106.0±1.5	16.0±3.0		
	80	118.0±0.2	4.6±0.7	167.1±0.5	14.8±1.2

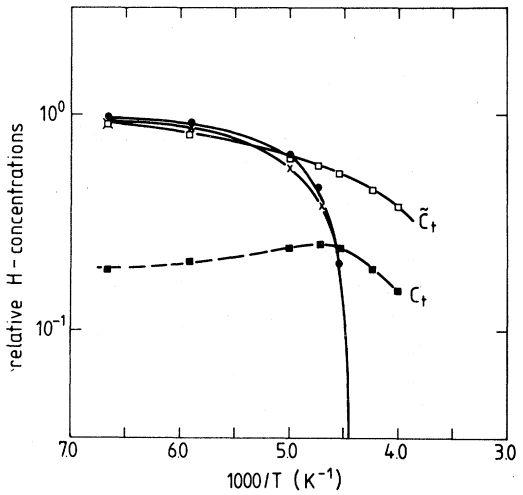

FIG. 4. Temperature dependence of the proton fractions in the trapped state and/or in the hydride phase as revealed from a fit with (i) a trapping model ($\tilde{C}_t$;□); (ii) a precipitation model (●); (iii) a combined precipitation and trapping model (C_t,■ trapped proton fraction, x sum of trapped and precipitated proton fraction).

tration in the dilute α phase is determined by the phase boundary with the hydride phase and is given by

$$C_\alpha = C_0 e^{-\Delta H/k_B T} , \tag{6}$$

where C_0 is a constant and ΔH is the enthalpy of formation of the hydride phase. Using this model, with C_0 and ΔH as fitting parameters, the results shown by the solid circles (●) in Fig. 4 were obtained. (Note that $C_P = C_H - C_\alpha$.) In contrast to the simple trapping model, this model predicts too rapid a transfer of intensity and does not account for the intensity near 125 meV observed at the higher temperatures (Fig. 3).

TABLE II. Parameters obtained from the simultaneous fit of the $Nb Cr_{0.009}H_{0.009}$ data.

Fit Parameter	Value (meV)	Error (meV)
α-phase peak:		
Position	108.1	0.3
FWHM	10.3	1.0
trapping peak		
Position	123.3	0.8
FWHM	6.2	2.2
Hydride-phase peak		
Position	116.7	0.3
FWHM	4.7	0.7
Binding Energy ΔE	105.0	10.0
Multiplicity of trap n	1.0[a]	

[a] n is badly defined and therefore was kept fixed in the fitting process. Changes of n do not significantly influence the results for the other parameters.

Therefore, we have combined the two models and assumed that both trapping and precipitation occur, i.e., that the binding energy of the trap is less than the enthalpy of formation of the hydride phase. At low temperatures, the concentration of hydrogen in the dilute phase will be governed by the phase boundary, assuming that the thermodynamic behavior of the precipitation is not affected by the presence of impurities.[15] Starting once again from Eq. (4) and noting that concentration in the dilute phase is now given by C_α as defined in Eq. (6), the trapped fraction C_t is given by

$$C_t = \frac{C_\alpha C_i}{C_i + (6/n)} e^{-\Delta E/k_B T} . \tag{7}$$

In order to minimize the number of parameters, the well-established values[16,3] of $C_0 = 4.7$ [H]/[Nb] and $\Delta H = 0.12$ meV were used for the fit, and ΔE was allowed to vary. The result of this fit is the one shown in Fig. 3 and the parameters obtained are given in Table II. The trapped-proton fraction and the sum of the trapped and precipitated fraction are given in Fig. 4 (C_t and x). It is evident from Fig. 3 that this combined model gives a good description of the data, both the slow onset of extra intensity at high temperatures, and the sudden increase in intensity of the high-energy peak near 210 K.

IV. DISCUSSION

The salient feature of the $NbTi_{0.01}H_{0.009}$ data is the complete absence of any peaks at the positions found in Ref. 12 for the hydride phase of Nb at 10 K. (The positions of the hydride-phase peaks are shown by arrows in Fig. 1.) Taking note of the fact that if the hydrogen were to precipitate into a hydride phase, the concentration of impurities in any precipitate would be less than 1% of the hydrogen concentration; this shows directly that the binding energy of the trap is larger than the enthalpy of formation of the hydride phase, so that precipitation is prevented. This result is in agreement with recent internal-friction measurements on[17] $NbTi_xH_y$ which revealed low-temperature relaxation peaks not found in pure NbH and which were therefore attributed to Ti-H pairs. In addition, the observed spectra are similar to what is predicted for a tetrahedral site, i.e., there are two fundamental energy levels, with the higher one being twofold degenerate. As was found for interstitial impurities,[12] the linewidths observed are larger than those observed for the hydride

phase at room temperature.[13,14] However, in contrast to the interstitial impurities, the substitutional Ti impurity does shift the energy levels down significantly from those observed in[18] pure Nb by approximately 2 ± 1.5 and 10 ± 3 meV for the lower and upper levels, respectively. This result could be explained by a general weakening of the near-neighbor metal-hydrogen force constants as a result of electronic changes induced by the Ti defect. As shown in Table I, the higher-energy peak is unusually broad even at 10 K, suggesting that the H occupies a distorted tetrahedral site which would lift the degeneracy of this level, e.g., one having a Ti nearest neighbor. However, we cannot reproduce the spectra by simply assuming an unperturbed Born-Mayer potential for the Nb-H interaction and an arbitrary Born-Mayer potential for the Ti-H interaction. Nonetheless, the large energy shift and width of the high-energy peak suggest that the H does occupy a near-neighbor site of the Ti, a result to be contrasted to that found for the interstitial impurities O and N, where the hydrogen occupies a more distant site.[12] This contrast in behavior is likely associated with the fact that the trapping by interstitial impurities is almost certainly strain-related, while for Ti, the trapping is likely electronic in origin. This follows from the observation that the elastic deformations caused by Ti in Nb are small,[19] $\Delta a/\Delta c = -0.32\times10^{-3}$ Å/at. %, compared to those for N or O ($\Delta a/\Delta c \sim 6.0\times10^{-3}$ and 4.1×10^{-3} Å/at. % respectively[20]), and thus the elastic interaction energies between Ti and H in Nb will be small. Given this, it is somewhat surprising that a trap deep enough to prevent hydride-phase precipitation leads to a *reduced* force constant, even allowing for the fact that the trap energy is related to the depth of the well while the force constant is related to its curvature.

The detailed analysis of the neutron line shapes for $NbCr_{0.009}H_{0.009}$ shows that Cr also provides a trapping site for H in Nb. We have extracted a value for both the binding energy of the trap and the shift of the lowest energy level in the trapped state. However, the multiplicity n of the traps was poorly defined and was set equal to one in the final fits with only minor effects on the values of the other parameters. The derived value for the binding energy of the trap is 105 meV, which is smaller than the enthalpy of formation of the hydride phase (120 meV). Thus at low temperatures the hydride phase precipitates out as shown by the spectrum obtained at 80 K (Fig. 1), which is very similar to that obtained for pure Nb-H in the ordered hydride phase. Although the shallow trap such as Cr in Nb does not prevent precipitation, it does seem to shift the solubility limit to lower temperatures compared to that in pure Nb, in this case by approximately 20 K. Our model gives this result directly and is also the most probable explanation of a similar shift observed in $NbV_{0.008}H_{0.005}$.[12]

In contrast to the case of Ti discussed above, Cr causes a large distortion of the Nb lattice $\Delta a/\Delta c = -5.69\times10^{-3}$ Å/at. %,[19] an amount similar to that caused by interstitial N or O traps. For the case of interstitial N and O traps, no shift of energy levels was observed, leading to the suggestion[12] that the hydrogen was trapped in a fourth-neighbor site of the impurity. At this distance, no effect of electronic changes in force constants would be expected, and thus we conclude that trapping is essentially due to the elastic interactions. Given this, it is somewhat surprising that Cr, with similar elastic distortions, does not give rise to a similar deep trap. However, systematic muon diffusion and trapping studies of Al doped with various substitutional impurities have shown that apparently no relation exists between trapping properties and long-range deformations,[21] e.g., it was found that impurities like Ag ($\Delta a/\Delta c \approx 0$) and Mn ($\Delta a/\Delta c = 1.5\times10^{-3}$) have essentially the same trapping characteristics.

Finally, we note that the position of the lowest-energy level in the trapped state for NbCr is shifted up by 15 meV relative to the pure metal or 14%. this is the largest effect on the vibrational spectrum observed for any trap. This result may be explained by the large elastic strains caused by Cr in Nb leading to a distorted environment near the Cr trap. According to recent calculations,[22] the Nb-H interaction is dominated by strong short-range repulsive forces, so that a reduction of the average Nb-H spacing would lead to a large increase in effective force constant.

V. CONCLUSION

These results demonstrate that inelastic neutron scattering is a powerful method to investigate the atomic scale mechanism and thermodynamics of the H trapping process in metals containing impurities, even for such an intricate case as *Nb*CrH where both trapping and hydride-phase precipitation occur.

We have found (i) Ti in Nb provides a strong trap for protons; (ii) in the trapped state the H site is approximately tetrahedral; (iii) the vibrational frequencies are shifted downwards compared to the α phase and the degenerate upper peak is broadened considerably; (iv) in contrast to Ti, Cr provides only shallow traps which do not inhibit hydride-phase precipitation; (v) the binding energy of the Cr traps is 105 ± 10 meV; (vi) the local mode-vibration frequency of the lower fundamental is increased by 14% at the trapping site, the largest impurity effect on the local modes so far observed.

ACKNOWLEDGMENTS

We would like to thank J. M. Welter and H. Bierfeld for their help during the sample preparation, H. Nickel for the chemical analysis, and R. Hempelmann for many valuable discussions. J. M. R. and D. R. acknowledge partial travel support by North Atlantic Treaty Organization (NATO) research grant No. 135.80.

[1]P. Kofstadt, W. E. Wallace, and L. J. Hyvönen, J. Am. Chem. Soc. 81, 5015, 5019 (1959).

[2]O. J. Kleppa, P. Dantzer, and M. E. Melnichak, J. Chem. Phys. 61, 4048 (1974).

[3]H. Pfeiffer and H. Wipf, J. Phys. F 6, 167 (1976).

[4]C. Baker and H. K. Birnbaum, Acta Metall. 21, 865 (1975).

[5]D. Richter and T. Springer, Phys. Rev. B 18, 126 (1978).

[6]P. E. Zapp and H. K. Birnbaum, Acta Metall. 28, 1275, 1523 (1980).

[7]C. Morkel, H. Wipf, and K. Neumeyer, Phys. Rev. Lett. 40, 947 (1978).

[8]D. B. Poker, G. G. Setser, A. V. Granato, and H. K. Birnbaum, Z. Phys. Chem. (Leipzig) NF 116, 39 (1979).

[9]H. Wipf, A. Magerl, S. M. Shapiro, S. K. Satija, and W. Thomlinson, Phys. Rev. Lett. 46, 947 (1981).

[10]D. Richter and H. Wipf (unpublished).

[11]This sensitivity has been demonstrated in earlier studies of metal-hydrogen systems. See, e.g., J. J. Rush and H. E. Flotow, J. Chem. Phys. 48, 3795 (1968); R. Khoda-Bakhsh and D. K. Ross, J. Phys. F 12, 15 (1982).

[12]A. Magerl, J. J. Rush, J. M. Rowe, D. Richter, and H. Wipf, Phys. Rev. B 27, 927 (1983).

[13]D. Richter and S. M. Shapiro, Phys. Rev. B 22, 599 (1980).

[14]J. J. Rush, A. Magerl, J. M. Rowe, J. M. Harris, and J. L. Provo, Phys. Rev. B 24, 4902 (1981).

[15]H. Y. Chang and C. A. Wert, Acta Metall. 21, 1233 (1973).

[16]G. Schaumann, J. Völkl, and G. Alefeld, Phys. Status Solidi 42, 401 (1970).

[17]G. Cannelli and R. Cantelli, Proceedings of the International Symposium on Metal-Hydrogen Systems, Miami Beach, 1981 (unpublished).

[18]Peak positions in α-$NbH_{0.005}$ at 295 K have recently been measured to be 106 ± 1 and 163 ± 3 meV; J. J. Rush, A. Magerl, and J. M. Rowe, private communication, also see Ref. 12.

[19]W. B. Pearson, *Lattice Spacings and Structure of Metals and Alloys* (Pergamon, Oxford, 1958).

[20]G. Hörz, in *Gase und Kohlenstoff in Metallen,* edited by E. Fromm and E. Gebhardt (Springer, Berlin, 1976).

[21]K. W. Kehr, D. Richter, J. M. Welter, O. Hartmann, E. Karlsson, L. O. Norlin, T. O. Niinikoski, and A. Yaouanc, Phys. Rev. B 26, 567 (1982).

[22]H. Sugimoto and Y. Fukai, Phys. Rev. B 22, 670 (1980).